

Role of the $qqqq\bar{q}$ components in the electromagnetic transition $\gamma^* N \rightarrow N^*(1535)$

C. S. An^{1,2} and B. S. Zou^{1,3}

¹ Institute of High Energy Physics, CAS, P.O.Box 918(4), Beijing 100049, China

² Helsinki Institute of Physics, POB 64, 00014 University of Helsinki, Finland

³ Theoretical Physics Center for Science Facilities, CAS, P.O.Box 918(4), Beijing 100049, China

Received: date / Revised version: date

Abstract. The helicity amplitudes $A_{1/2}^p$ and $S_{1/2}^p$ for the electromagnetic transition $\gamma^* N \rightarrow N^*(1535)$ are calculated in the quark model that is extended to include the lowest lying $qqqq\bar{q}$ components in addition to the qqq component. It is found that with admixture of 5-quark components with a proportion of 20% in the nucleon and 25-65% in the $N^*(1535)$ resonance the calculated helicity amplitude $A_{1/2}^p$ decreases at the photon point, $Q^2 = 0$ to the empirical range. The $qqqq\bar{q}$ components contain $s\bar{s}$ pairs, which is consistent with the substantial width for $N\eta$ decay of the $N^*(1535)$. The best description of the momentum dependence of the empirical helicity amplitudes is obtained by assuming that the $qqqq\bar{q}$ components are more compact than the qqq component. However, this version of extended quark model still does not lead to a satisfactory simultaneous description of both $A_{1/2}^p$ and $S_{1/2}^p$ although with significant improvement.

PACS. 12.39.Jh Nonrelativistic quark model – 14.20.Gk Baryon resonances with $S=0$

1 Introduction

The structure of the nucleon resonances with spin-parity $1/2^-$ has continued to be somewhat enigmatic. On the one hand the number of observed resonances coincides with that predicted by the constituent quark model with a monotonic confining interaction [1, 2], while on the other hand several of these resonances can be dynamically generated in chiral meson-nucleon models [3, 4]. The question then is whether a 3 quark or a 4 quark + 1 antiquark description is the more appropriate one. The $N^*(1535)$ resonance is particularly interesting in this regard, as it has a sizeable $N\eta$ decay branch, even though its energy is very close to the threshold of that decay. The electromagnetic transition form factors of this resonance may in fact contain crucial information to settle this issue. It has recently been shown that the chiral dynamical approach can provide a description of both the $A_{1/2}^p$ and the $S_{1/2}^p$ transition form factors [5], while a simultaneous description of both these form factors has proven elusive in the basic qqq constituent quark model [6].

To bridge the gap between the constituent quark model and the chiral meson-nucleon resonance models, it is natural to extend the former to include explicit $qqqq\bar{q}$ components in addition to its basic qqq structure. In the case of the $\Delta(1232)$ and the $N^*(1440)$ resonances it has been shown that already a modest admixture of $qqqq\bar{q}$ components can remove the main under-prediction of the de-

cay widths that is typical of the qqq quark model [7, 8, 9]. Moreover, it has recently been shown that the coupling of $N^*(1535)N\phi$ may be significant [10], which is consistent with the previous indications of the notable $N^*(1535)K\Lambda$ coupling [11]. These suggest that there are large $s\bar{s}$ components in the $N^*(1535)$ resonance. With this suggestion, we can give a natural explanation of the mass ordering of the $N^*(1440)1/2^+$, $N^*(1535)1/2^-$ and $\Lambda^*(1405)1/2^-$ resonances [11].

Here we calculate the helicity transition amplitudes $A_{1/2}^p$ and $S_{1/2}^p$ for the electromagnetic transition $\gamma^* p \rightarrow N^*(1535)$, by including contributions from both qqq components and those $qqqq\bar{q}$ components with configurations expected to have the lowest energy in the proton and $N^*(1535)$. These amplitudes are not well described in the conventional qqq constituent quark model [12, 13]. The results show that the calculated transition amplitudes can be improved by taking inclusion of the $qqqq\bar{q}$ components.

We take the flavor-spin configurations of the four-quark subsystem in the $qqqq\bar{q}$ components in the proton to be $[4]_{FS}[22]_F[22]_S$, which is likely to have the lowest energy [14]. In the case of the negative parity $N^*(1535)$ resonance the corresponding most likely lowest energy configuration is $[31]_{FS}[211]_F[22]_S$ [14]. The flavor configuration $[211]_F$ in the latter requires that the $qqqq\bar{q}$ component can only be $qqqs\bar{s}$. This implies a large hidden strangeness in the $N^*(1535)$ resonance and strong couplings to $N\phi$ and $K\Lambda$ states, which is consistent with the results in Refs.

[10] and [11]. This feature is also in line with the mechanism of dynamical resonance formation within the coupled channel approach based on chiral $SU(3)$ with the $K\Sigma$ quasi-bound state explanation for the $N^*(1535)$ [3, 4, 5, 15, 16]. For completeness we also consider the contributions of $d\bar{d}$ or $u\bar{u}$ components in the $N^*(1535)$ and consequently, which appear in the next-to-next-to-lowest-energy configuration [31]_{FS}[22]_F[31]_S.

Some of the empirical results on the strangeness magnetic form factors may be described, at least qualitatively, by $uuds\bar{s}$ configurations in the proton, where the \bar{s} antiquark is in the S -state [17, 18]. Since configurations with the antiquark in the S -state cannot be represented by long range pion or kaon loop fluctuations, this motivates to a systematic extension of the qqq quark model to include the $qqqq\bar{q}$ configurations explicitly. On the other hand, the overall descriptions of the baryon magnetic moments may be improved by taking the $qqqq\bar{q}$ components contributions into account [19, 20].

This present manuscript is organized in the following way. The wave functions of the proton and $N^*(1535)$ are given in section 2. The helicity amplitudes $A_{1/2}^p$ and $S_{1/2}^p$ for $\gamma^* p \rightarrow N^*(1535)$ are calculated in section 3. Finally section 4 contains a concluding discussion.

2 The wave functions of nucleon and $N^*(1535)$

The internal nucleon wave functions that include $qqqq\bar{q}$ components in addition to the conventional qqq components for the proton and $N^*(1535)$ may be written in the following form:

$$\begin{aligned} |P, s_z\rangle &= A_{(P)3q}|qqq\rangle + A_{(P)5q} \sum_i A_i |qqqq\bar{q}_i\rangle, \\ |N^*(1535), s_z\rangle &= A_{(N^*)3q}|qqq\rangle + A_{(N^*)5q} \\ &\quad \times \sum_i A_i |qqqq\bar{q}_i\rangle. \end{aligned} \quad (1)$$

Here $A_{(P)3q}$ and $A_{(P)5q}$ are the amplitudes for the 3-quark and 5-quark components in the nucleon, respectively; $A_{(N^*)3q}$ and $A_{(N^*)5q}$ are the corresponding factors for $N^*(1535)$. The sum over i runs over all the possible $qqqq\bar{q}_i$ components, and the factors A_i denotes the corresponding coefficient for the $qqqq\bar{q}_i$ component. We give the explicit forms of the qqq and $qqqq\bar{q}$ components in the proton and $N^*(1535)$ in the next two subsections.

2.1 The wave functions of qqq components

Here we take the wave functions for the qqq components in proton and $N^*(1535)$ to be the conventional ones, which can be expressed in the following way in the harmonic oscillator quark model:

$$|P, s_z\rangle_{3q} = \frac{1}{\sqrt{2}}(|\frac{1}{2}, t_z\rangle_+ |\frac{1}{2}, s_z\rangle_+ + |\frac{1}{2}, t_z\rangle_- |\frac{1}{2}, s_z\rangle_-)$$

$$\begin{aligned} &\times \phi_{00}(\boldsymbol{\kappa}_2) \phi_{00}(\boldsymbol{\kappa}_1), \\ |N^*(1535), s_z\rangle_{3q} &= \frac{1}{2} \sum_{ms} C_{1m, \frac{1}{2}, s}^{\frac{1}{2}, s_z} \{ \phi_{1m}(\boldsymbol{\kappa}_2) \phi_{00}(\boldsymbol{\kappa}_1) [|\frac{1}{2}, t_z\rangle_+ |\frac{1}{2}, s\rangle_+ \\ &\quad - |\frac{1}{2}, t_z\rangle_- |\frac{1}{2}, s\rangle_-] - \{ \phi_{00}(\boldsymbol{\kappa}_2) \phi_{1m}(\boldsymbol{\kappa}_1) [|\frac{1}{2}, t_z\rangle_+ \\ &\quad \times |\frac{1}{2}, s\rangle_- + |\frac{1}{2}, t_z\rangle_- |\frac{1}{2}, s\rangle_+] \}. \end{aligned} \quad (2)$$

Here $|\frac{1}{2}, s_z\rangle_\pm$ and $|\frac{1}{2}, t_z\rangle_\pm$, with t_z being the z-component of the isospin, are spin and isospin wave functions of mixed symmetry [21]_S and [21]_F, respectively, in which '+' denotes a state that is symmetric and '-' denotes a state that is anti-symmetric under exchange of the spin or isospin of the first two quarks. The momenta $\boldsymbol{\kappa}_i$ are defined by the three quarks momenta as

$$\begin{aligned} \boldsymbol{\kappa}_1 &= \frac{1}{\sqrt{2}}(\mathbf{p}_1 - \mathbf{p}_2), \\ \boldsymbol{\kappa}_2 &= \frac{1}{\sqrt{6}}(\mathbf{p}_1 + \mathbf{p}_2 - 2\mathbf{p}_3). \end{aligned} \quad (3)$$

The harmonic oscillator wave functions are

$$\phi_{00}(\boldsymbol{\kappa}; \omega_3) = \frac{1}{(\omega_3^2 \pi)^{3/4}} \exp\{-\frac{\boldsymbol{\kappa}^2}{2\omega_3^2}\}, \quad (4)$$

$$\phi_{1, \pm 1}(\boldsymbol{\kappa}; \omega_3) = \mp \sqrt{2} \frac{\kappa_\pm}{\omega_3} \phi_{00}(\boldsymbol{\kappa}; \omega_3), \quad (5)$$

$$\phi_{10}(\boldsymbol{\kappa}; \omega_3) = \sqrt{2} \frac{\kappa_0}{\omega_3} \phi_{00}(\boldsymbol{\kappa}; \omega_3). \quad (6)$$

Here $\kappa_\pm \equiv \frac{1}{\sqrt{2}}(\kappa_x \pm i\kappa_y)$, and $\kappa_0 \equiv \kappa_z$. The subscripts denote the quantum numbers (lm) of the oscillator wave functions.

2.2 The wave functions of $qqqq\bar{q}$ components

If the hyperfine interaction between the quarks depends on spin and flavor [2], the $qqqq$ subsystems of the $qqqq\bar{q}$ components with the mixed spatial symmetry [31]_X are expected to be the configurations with the lowest energy, and therefore most likely to form appreciable components of the baryons with positive parity. Consequently the flavor-spin state of the $qqqq$ subsystem is most likely totally symmetric: [4]_{FS}. Moreover in the case of the proton, the flavor-spin configuration of the four quark subsystem [4]_{FS}[22]_F[22]_S, with one quark in its first orbitally excited state, and the anti-quark in its ground state, is likely to have the lowest energy [14], consequently, the $qqqq\bar{q}_i$ components and the corresponding amplitudes in the proton may be [19]:

$$\sqrt{\frac{2}{3}}|[uudd]_{[22]_F}\bar{d}\rangle + \sqrt{\frac{1}{3}}|[uuds]_{[22]_F}\bar{s}\rangle. \quad (7)$$

The explicit form of the wave functions for these two $q\bar{q}$ components may be expressed as [18, 19, 9]:

$$|p, s_z\rangle_{5q} = \frac{1}{\sqrt{2}} \sum_{a,b} \sum_{m,s} C_{1m, \frac{1}{2}, s}^{\frac{1}{2}, s_z} C_{[31]_a [211]_a}^{[14]} [211]_C(a) [31]_{X,m}(a)$$

$$\times [22]_F(b)[22]_S(b)\bar{\chi}_s\psi(\boldsymbol{\kappa}_i).$$

Here the flavor-spin, color and orbital wave functions of the $qqqq$ subsystem have been denoted by the Young patterns, respectively. The sum over a runs over the three configurations of the $[31]_X$ and $[211]_C$ representations of S_4 permutation group, and the sum over b runs over the two configurations of the $[22]_F$ and $[22]_S$ representations of S_4 permutation group, respectively. The factors $C_{[31]_a[211]_a}^{[1^4]}$ denotes the S_4 Clebsch-Gordan coefficients.

The explicit forms of the flavor-spin configurations have been given in Ref. [18], and the explicit color-space part of the wave function (8) may be expressed in the form [9]:

$$\begin{aligned} \psi_C(\{\boldsymbol{\kappa}_i\}) = & \frac{1}{\sqrt{3}} \{ [211]_C \varphi_{1m}(\boldsymbol{\kappa}_1) \varphi_{00}(\boldsymbol{\kappa}_2) \varphi_{00}(\boldsymbol{\kappa}_3) - [211]_C \\ & \times \varphi_{00}(\boldsymbol{\kappa}_1) \varphi_{1m}(\boldsymbol{\kappa}_2) \varphi_{00}(\boldsymbol{\kappa}_3) + [211]_C \\ & \times \varphi_{00}(\boldsymbol{\kappa}_1) \varphi_{00}(\boldsymbol{\kappa}_2) \varphi_{1m}(\boldsymbol{\kappa}_3) \} \varphi_{00}(\boldsymbol{\kappa}_4). \end{aligned} \quad (9)$$

Here the two additional Jacobi momenta $\boldsymbol{\kappa}_3$ and $\boldsymbol{\kappa}_4$ are defined as

$$\boldsymbol{\kappa}_3 = \frac{1}{\sqrt{12}}(\mathbf{p}_1 + \mathbf{p}_2 + \mathbf{p}_3 - 3\mathbf{p}_4), \quad (10)$$

$$\boldsymbol{\kappa}_4 = \frac{1}{\sqrt{20}}(\mathbf{p}_1 + \mathbf{p}_2 + \mathbf{p}_3 + \mathbf{p}_4 - 4\mathbf{p}_5). \quad (11)$$

and the harmonic oscillator wave functions are

$$\varphi_{00}(\boldsymbol{\kappa}; \omega_5) = \frac{1}{(\omega_5^2 \pi)^{3/4}} \exp\left\{-\frac{\boldsymbol{\kappa}^2}{2\omega_5^2}\right\}, \quad (12)$$

$$\varphi_{1,\pm 1}(\boldsymbol{\kappa}; \omega_5) = \mp \sqrt{2} \frac{\kappa_{\pm}}{\omega_5} \varphi_{00}(\boldsymbol{\kappa}; \omega_5), \quad (13)$$

$$\varphi_{10}(\boldsymbol{\kappa}; \omega_5) = \sqrt{2} \frac{\kappa_0}{\omega_5} \varphi_{00}(\boldsymbol{\kappa}; \omega_5). \quad (14)$$

In the case of the wave functions for the $qqqq\bar{q}$ components in the S_{11} resonance $N^*(1535)$, the parity of which is negative, are definitely not same as that of the proton. Negative parity demands that all of the quarks and the anti-quark be in their ground state, or states with higher even angular momentum. If the flavor- and spin-dependent hyperfine interaction between the quarks are employed, for the $qqqq$ subsystem, the flavor-spin configuration $[31]_{FS}[211]_F[22]_S$ is expected to have the lowest energy, and the orbital state should be completely symmetric state $[4]_X$ [14]. Consequently, the wave function of the $qqqq\bar{q}$ component in $N^*(1535)$ may be expressed as

$$\begin{aligned} |N^*(1535), s_z\rangle_{5q} = & \sum_{abc} C_{[31]_a[211]_a}^{[1^4]} C_{[211]_b[22]_c}^{[31]_a} [4]_X [211]_F(b) \\ & \times [22]_S(c) [211]_C(a) \bar{\chi}_{s_z} \varphi(\{\boldsymbol{\kappa}_i\}). \end{aligned} \quad (15)$$

Note that the total spin of the four quark subsystem with symmetry $[22]_S$ is $S = 0$. The flavor configuration $[211]_F$ implies that the $qqqq\bar{q}$ components can only be $uuds\bar{s}$. Consequently there are appreciable $s\bar{s}$ components in $N^*(1535)$, which is consistent with the strong coupling of $N^*(1535)K\Lambda$ [11] and $N^*(1535)N\phi$ [10]. From this assumption it follows that the proportion of the $s\bar{s}$ in the

(8) $N^*(1535)$ resonance might equal P_{5q} . In the Roper resonance, the probability of the $s\bar{s}$ component would then be only $P_{5q}/3$ [19]. If we set same probability P_{5q} of the $qqqq\bar{q}$ components in $N^*(1535)$ and $N^*(1440)$ the larger proportion of the strange component may then make $N^*(1535)$ heavier than the Roper resonance as desired. This has been a puzzle in the conventional qqq constituent quark model with flavor independent hyperfine interactions.

In addition, there may be smaller $d\bar{d}$ or $u\bar{u}$ components in $N^*(1535)$. The next-to-lowest-energy $qqqq\bar{q}$ configuration is however in this scheme $[4]_X[31]_{FS}[211]_F[31]_S$ [14], which also rules out the $u\bar{u}$ and $d\bar{d}$ components. The contributions to the electromagnetic transition $\gamma^* p \rightarrow N^*(1535)$ of this configuration may be replaced by that of certain proportion of the lowest energy $qqqq\bar{q}$ component. Consequently, one has to consider the configuration with $qqqq$ subsystem of the orbital-flavor-spin symmetry $[4]_X[31]_{FS}[22]_F[31]_S$, which is the lowest energy configuration allowing $uudd\bar{d}$ component with spin-parity $J^P = 1/2^-$ [14]. For this configuration, the $qqqq\bar{q}_i$ components and the amplitudes in the $N^*(1535)$ may be [19]:

$$\sqrt{\frac{2}{3}}|[uudd]_{[22]_F}\bar{d}\rangle + \sqrt{\frac{1}{3}}|[uuds]_{[22]_F}\bar{s}\rangle. \quad (16)$$

The explicit form of the wave function for these two $q\bar{q}$ components may be expressed as:

$$\begin{aligned} |N^*(1535), s_z\rangle_{5q'} = & \sum_{abc} C_{[31]_a[211]_a}^{[1^4]} C_{[211]_b[22]_c}^{[31]_a} [4]_X [22]_F(b) \\ & \times [31]_S(c) [211]_C(a) \bar{\chi}_{s_z} \varphi(\{\boldsymbol{\kappa}_i\}). \end{aligned} \quad (17)$$

Actually, we can also obtain the probabilities of the $qqqq\bar{q}$ components from a recent manuscript [21]. The vanishing or small axial charge of $N^*(1535)$ requires that there should be a cancelation between the contributions of the qqq and $qqqq\bar{q}$ components. Consequently, the most obvious five-quarks components should be the ones in which the flavor-spin configurations of the four-quarks subsystem are $[31]_{FS}[211]_F[22]_S$, $[31]_{FS}[211]_F[31]_S$ or $[31]_{FS}[31]_F[31]_S$. And the large coefficients A_n obtained from the latter two configurations indicate that the probabilities of these two components should be smaller than the first one.

3 The electromagnetic transition

$\gamma^* N \rightarrow N^*(1535)$

The calculation of the helicity amplitudes $A_{1/2}^p$ and $S_{1/2}^p$ for the electromagnetic transition $\gamma^* p \rightarrow N^*(1535)$ that takes into account the contributions of the $qqqq\bar{q}$ components discussed above falls into three parts: (1) the contributions of the direct transition $\gamma^* qqq \rightarrow qqq$, i. e. the contributions of the qqq components in proton and $N^*(1535)$, (2) the contributions of the lowest energy $qqqq\bar{q}$ component in $N^*(1535)$, and (3) the contributions of the next-to-next-to-lowest-energy $qqqq\bar{q}$ component in $N^*(1535)$. And each of the latter two parts contains contributions from two processes: the direct transition $\gamma^* qqqq\bar{q} \rightarrow qqqq\bar{q}$, i.e.

the diagonal transitions, and the annihilation transition $\gamma^* qqq \rightarrow qqq\bar{q}$ (or $\gamma^* qqq\bar{q} \rightarrow qqq$), i.e. the off-diagonal transitions.

In the non-relativistic approximation the elastic and annihilation current operators are:

$$\begin{aligned}\langle \mathbf{p}' | j^0 | \mathbf{p} \rangle_{elas} &= 1, \\ \langle \mathbf{p}' | j^0 | \mathbf{p} \rangle_{anni} &= \frac{1}{2m} [\boldsymbol{\sigma} \cdot (\mathbf{p}' + \mathbf{p})], \\ \langle \mathbf{p}' | \mathbf{j} | \mathbf{p} \rangle_{elas} &= \frac{\mathbf{p}' + \mathbf{p}}{2m} + \frac{i}{2m} (\boldsymbol{\sigma} \times \mathbf{q}), \\ \langle \mathbf{p}' | \mathbf{j} | \mathbf{p} \rangle_{anni} &= \boldsymbol{\sigma},\end{aligned}\quad (18)$$

respectively. Here we have set $\mathbf{q} = \mathbf{p}' - \mathbf{p}$.

3.1 The contributions of the qqq components to the helicity amplitude $A_{1/2}^P$ and $S_{1/2}^P$

For point-like quarks the electromagnetic transition operator for elastic transitions between states with n_q quarks is

$$\begin{aligned}\hat{T}_A &= - \sum_{i=1}^{n_q} \frac{e_i}{2m_i} [\sqrt{2} \hat{\sigma}_{i+} k_\gamma + (p'_{i+} + p_{i+})] \\ \hat{T}_S &= \sum_{i=1}^{n_q} e_i.\end{aligned}\quad (19)$$

Here \hat{T}_A and \hat{T}_S are the corresponding operators for the transverse and longitudinal helicity amplitudes, which are obtained by coupling the current operators (18) to the transverse ($\epsilon_{+1} = -\frac{1}{\sqrt{2}}(\hat{x} + i\hat{y})$ and $\epsilon_0 = 0$) and longitudinal ($\epsilon = 0$ and $\epsilon_0 = 1$) photon [22], respectively. And e_i and m_i denote the electric charge and constituent mass of the quark which absorbs the photon, respectively. p_{i+} and p'_{i+} are defined as the initial and final momenta of the quark that absorbs the photon:

$$p'_{i+} \equiv \frac{1}{\sqrt{2}}(p'_{ix} + ip'_{iy}), \quad (20)$$

and $\hat{\sigma}_{i+}$ is defined as

$$\hat{\sigma}_{i+} \equiv \frac{1}{2}(\hat{\sigma}_{ix} + i\hat{\sigma}_{iy}), \quad (21)$$

which raises the spin of the quark which absorbs the photon. Here we consider a right-handed virtual-photon in the operator \hat{T}_A , and the momentum of photon has been set to be: $\mathbf{k} = (0, 0, k_\gamma)$ in the center-of-mass frame of the final resonance $N^*(1535)$. It is related to the initial and final momentum of the quark which absorbs the photon as $k_\gamma = \mathbf{p}'_i - \mathbf{p}_i$, and the magnitude of four-momentum transfer $Q = \sqrt{-k^2}$ as:

$$k_\gamma^2 = Q^2 + \frac{(M^{*2} - M_N^2 - Q^2)^2}{4M^{*2}}, \quad (22)$$

where M^* and M_N denote the mass of $N^*(1535)$ resonance and proton, respectively.

With the diagonal transition operators (19), the helicity amplitudes of the electromagnetic transition $\gamma^* p \rightarrow N^*(1535)$, which include only the contributions from the qqq components in the proton and the $N^*(1535)$, may be expressed as

$$\begin{aligned}A_{1/2}^P &= \frac{1}{\sqrt{2K_\gamma}} \langle N^*(1535), \frac{1}{2}, \frac{1}{2} | \hat{T}_A | p, \frac{1}{2}, -\frac{1}{2} \rangle, \\ S_{1/2}^P &= \frac{1}{\sqrt{2K_\gamma}} \langle N^*(1535), \frac{1}{2}, \frac{1}{2} | \hat{T}_S | p, \frac{1}{2}, \frac{1}{2} \rangle.\end{aligned}\quad (23)$$

Here K_γ is the real-photon three-momentum in the center of mass frame of $N^*(1535)$.

With the wave functions (2) and the operators (19), we can obtain the helicity amplitudes $A_{1/2}^P$ and $S_{1/2}^P$ in the following form:

$$\begin{aligned}A_{1/2}^{p(3q)} &= A_{(p)3q} A_{(N^*)3q} \frac{1}{\sqrt{2K_\gamma}} \frac{e}{2m} \left(\frac{k_\gamma^2}{3\omega_3} + \frac{2\omega_3}{3} \right) \exp\left\{-\frac{k_\gamma^2}{6\omega_3^2}\right\} \\ S_{1/2}^{p(3q)} &= -A_{(p)3q} A_{(N^*)3q} \frac{1}{\sqrt{2K_\gamma}} \frac{e}{3\sqrt{2}} \frac{k_\gamma}{\omega_3} \exp\left\{-\frac{k_\gamma^2}{6\omega_3^2}\right\}.\end{aligned}\quad (24)$$

Here e denotes the electric charge of the proton. The model parameters are the constituent masses of the light quarks m , the oscillator parameter ω_3 , and the qqq components amplitudes A_{3q} . For the qqq model, we set the constituent quark mass to be $m = 340$ MeV. The oscillator parameter ω_3 may be determined by the nucleon radius as $\omega_3 = \frac{1}{\sqrt{\langle r^2 \rangle}}$, which yield the value 246 MeV, while the empirical value for this parameter falls in the range 110 – 410 MeV [9,24]. We give the numerical results as functions of Q^2 by setting $\omega_3 = 340$ MeV, $\omega_3 = 246$ MeV and $\omega_3 = 200$ MeV, respectively, which are shown in figure 1 and 2 for the transverse and longitudinal helicity amplitudes, respectively, compared to the experimental data extracted from Ref. [25,26,27]. As in this case there are no $qqq\bar{q}$ components in the proton and $N^*(1535)$ the amplitudes are $A_{(p)3q} = A_{(N^*)3q} = 1$.

As shown in figure 1, none of the three curves can describe the experimental data satisfactorily. At the photon point, $Q^2 = 0$, the calculated helicity amplitudes are $A_{1/2}^P = 0.147/\sqrt{\text{GeV}}$ and $A_{1/2}^P = 0.115/\sqrt{\text{GeV}}$ with the parameter $\omega_3 = 340$ MeV and $\omega_3 = 246$ MeV, respectively, both of which are larger than the experimental value $A_{1/2}^P = 0.090 \pm 0.030/\sqrt{\text{GeV}}$ [25]. For the curve which is obtained by setting the parameter $\omega_3 = 200$ MeV, the calculated amplitude describes the data better at the photon point, but it falls too fast in comparison with the data when Q^2 increases. Similarly in the case of the longitudinal helicity amplitude $S_{1/2}^P$, none of the three curves can fit the data well, as that all of them are too small near the photon point.

3.2 The contributions of the lowest energy $qqqq\bar{q}$ components of $N^*(1535)$ to the helicity amplitude $A_{1/2}^P$ and $S_{1/2}^P$

The contributions of the $qqqq\bar{q}$ components contain the direct transition matrix elements $\gamma^* qqqq\bar{q} \rightarrow qqqq\bar{q}$, and the annihilation transition elements $\gamma^* qq\bar{q} \rightarrow qqqq\bar{q}$ and $\gamma^* qqqq\bar{q} \rightarrow qq\bar{q}$, i. e. the diagonal and non-diagonal transitions.

The contributions from the diagonal transition elements of the $qqqq\bar{q}$ components are obtained as matrix elements of the operator (19) (with $n_q = 5$) between the $5q$ wave functions (8) and (15), and between the wave functions (8) and (17). At the first step, we consider the contributions of the lowest energy $qqqq\bar{q}$ components in $N^*(1535)$.

The lowest energy configuration in the $qqqq\bar{q}$ components in $N^*(1535)$ is the one in which the flavor-spin configuration of the four quark subsystem has the mixed symmetry $[31]_{FS}[211]_F[22]_S$, as mentioned in section 2. For the spin symmetry $[22]_S$ ($S = 0$), both in the proton and $N^*(1535)$, the matrix elements of the operator $\hat{\sigma}_{i+}$ of these four quarks vanish. On the other hand, by the orthogonality of the four-quark orbital states $[31]_X$ (for the proton) and $[4]_X$ (for the $N^*(1535)$), the matrix element of the operator \hat{T}_A of the anti-quark does not contribute to the transition $\gamma^* qqqq\bar{q} \rightarrow qqqq\bar{q}$. Finally the contributions to $A_{1/2}^{p(5q)}$ only come from the matrix element of the second term of the operator \hat{T}_A (19) between the four quark states. In the case of the helicity amplitude $S_{1/2}^{p(5q)}$, the matrix element of the operator should vanish for the orthogonality of the different $qqqq\bar{q}$ states in proton and $N^*(1535)$.

Explicit calculation yields:

$$A_{1/2}^{p(5q)} = A_{(p)s\bar{s}} A_{(N^*)s\bar{s}} \frac{1}{\sqrt{2K_\gamma}} \frac{\omega_5}{24} \left(\frac{e}{2m} - \frac{e}{2m_s} \right) \exp\left\{-\frac{k_\gamma^2}{5\omega_5^2}\right\}$$

$$S_{1/2}^{p(5q)} = 0. \quad (25)$$

Here we have neglected the transition between the $uudd\bar{d}$ component in the proton and the $uuds\bar{s}$ component in $N^*(1535)$, which should be very tiny.

Consider the contributions of the non-diagonal transition elements, i. e. the transitions $\gamma^* qq\bar{q} \rightarrow qqqq\bar{q}$ and $\gamma^* qqqq\bar{q} \rightarrow qq\bar{q}$. By equation (18), the operator for these transitions may be expressed as

$$\hat{T}_{Aanni} = - \sum_{i=1}^4 \sqrt{2} e_i \hat{\sigma}_{i+},$$

$$\hat{T}_{Sanni} = \sum_{i=1}^4 \frac{e_i}{2m_i} \boldsymbol{\sigma} \cdot (\mathbf{p}_i + \mathbf{p}_5). \quad (26)$$

Here \hat{T}_{Aanni} and \hat{T}_{Sanni} denote the transition operators for $A_{1/2}^{p(anni)}$ and $S_{1/2}^{p(anni)}$, respectively, and e_i and m_i are the electric charge and the constituent mass of the annihilating quark, and $\hat{\sigma}_{i+}$ raises the spin of the corresponding

quark. \mathbf{p}_i is the momentum of the annihilating quark and \mathbf{p}_5 the momentum of the antiquark.

First, we calculate the matrix elements for the transitions $\gamma^* qq\bar{q} \rightarrow qqqq\bar{q}$. These involve calculations of the overlap between the $\gamma^* qq\bar{q}$ wave function and that for the $qqqq\bar{q}$ component in $N^*(1535)$.

In the case of the lowest energy configurations, the flavor-spin configuration has the mixed symmetry $[31]_{FS}[211]_F[22]_S$, the explicit form of which is shown in appendix A. For the case of the color overlap, the only contribution comes from the color symmetry configuration of the $qqqq\bar{q}$ component in $N^*(1535)$ which is denoted by $[211]_{C3}$. The matrix elements between the color singlet of the qqq component in the proton and the other two color configurations ($[211]_{C1}$ and $[211]_{C2}$) vanish.

Explicit calculation leads to the result:

$$A_{1/2}^{p(3q \rightarrow 5q)} = -A_{(p)3} A_{(N^*)s\bar{s}} \frac{1}{\sqrt{2K_\gamma}} \frac{\sqrt{2}}{6} e C_{35} \exp\left\{-\frac{3k_\gamma^2}{20\omega_5^2}\right\},$$

$$S_{1/2}^{p(3q \rightarrow 5q)} = A_{(p)3} A_{(N^*)s\bar{s}} \frac{1}{\sqrt{2K_\gamma}} \frac{1}{6} \frac{e}{2m_s} k_\gamma C_{35}$$

$$\times \exp\left\{-\frac{3k_\gamma^2}{20\omega_5^2}\right\}. \quad (27)$$

Here the factor C_{35} denotes the orbital overlap factor:

$$\langle \varphi_{00}(\mathbf{\kappa}_1) \varphi_{00}(\mathbf{\kappa}_2) | \varphi_{00}(\mathbf{\kappa}_1) \varphi_{00}(\mathbf{\kappa}_2) \rangle = \left(\frac{2\omega_3\omega_5}{\omega_3^2 + \omega_5^2} \right)^3. \quad (28)$$

Here we have obtained the helicity amplitudes $A_{1/2}^P$ and $S_{1/2}^P$ for the electromagnetic transition $\gamma^* p \rightarrow N^*(1535)$, which contains the contributions both of the qqq and the lowest energy $qqqq\bar{q}$ components in the proton and $N^*(1535)$. The results are shown in figure 3 and 4, respectively. Here we have taken the probability of the $qqqq\bar{q}$ components in the proton as the tentative value $P_{5q} = 20\%$, and in $N^*(1535)$ $P_{5q} = 45\%$. Taking the $qqqq\bar{q}$ components into account, the constituent quarks masses should be a bit smaller than the ones we employ in the previous section. To reproduce the mass for the nucleon when the five-quark components have been included, we take the values $m_u = m_d = m = 290$ MeV, and $m_s = 430$ MeV. The oscillator parameters are ω_3 and ω_5 . The latter one is treated as a free parameter in this manuscript. Note that the value for the ω_5 may be different from that for ω_3 . In our extended quark model with each baryon as a mixture of the three-quark and five-quark components, the two components represent two different states of the baryon. For the $qqqq\bar{q}$ state, there are more color sources than the qqq state, and may make the effective phenomenological confinement potential stronger. This is consistent with other empirical evidence favoring larger value of the ω_5 [7, 8, 9, 19]. An intuitive picture for our extended quark model is like this: the qqq state has weaker potential; when quarks expand, a $q\bar{q}$ pair is pulled out and results in a $qqqq\bar{q}$ state with stronger potential; the stronger potential leads to a more compact state which then makes the \bar{q} to annihilate with a quark easily and transits to the qqq state; this

leads to constantly transitions between these two states. Here presented are the results by setting $\omega_3 = 340$ MeV and $\omega_5 = 600$ MeV, $\omega_3 = 246$ and $\omega_5 = 600$ MeV, and $\omega_3 = 340$ MeV and $\omega_5 = 1000$ MeV, respectively. As shown in figure 3, the results describe the experimental data for $A_{1/2}^p$ well when the oscillator parameters are given the values $\omega_3 = 340$ MeV and $\omega_5 = 600$ MeV, both at the photon point and larger Q^2 . While in figure 4, the magnitude of the values for $S_{1/2}^p$ are however larger than the experimental value, even though the momentum dependence appears reasonable. Intriguingly when Q^2 increases to about 1.8GeV^2 the calculated values change sign. So here we should conclude that this model can work when the Q^2 is less than 1.8GeV^2 , if Q^2 is larger than this value, maybe we should consider the relativistic effect.

There are another important parameter in our model, the phase factors δ between the qqq and $qqqq\bar{q}$ components of the $N^*(1535)$ resonance, which has been taken to be $+1$. But in principle, this factor could be an arbitrary complex one $\exp\{i\phi\}$. As we know, the helicity amplitude $A_{1/2}^p$ is real, so here we may choose δ to be ± 1 . And as shown in figure 3, the non-diagonal transition contributes a minus value to the $A_{1/2}^p$. If we assume δ to be -1 , the numerical value for $A_{1/2}^p$ may be about $0.110/\sqrt{\text{GeV}}$, the result is not so good. Consequently, the best choice for us may be $\delta = +1$.

Note that the diagonal contributions of the lowest energy $qqqq\bar{q}$ component in $N^*(1535)$ to $S_{1/2}^p$ is 0. Actually, the contributions of the diagonal transition to $A_{1/2}^p$ are also very small, which is less than $0.01/\sqrt{\text{GeV}}$. But the non-diagonal contributions are significant, and negative for $A_{1/2}^p$ and positive for $S_{1/2}^p$, which are shown in figure 3 and 4 by the dash dot curves, with the parameter values $\omega_3 = 340$ MeV and $\omega_5 = 600$ MeV. For instance, at the photon point, $Q^2 = 0$, with the parameter values $\omega_3 = 340$ MeV and $\omega_5 = 600$ MeV, the contribution to $A_{1/2}^p$ is about $-0.025/\sqrt{\text{GeV}}$, which can decrease the helicity amplitude $A_{1/2}^p$ to describe the data.

3.3 The contributions of the next-to-next-to-lowest-energy $qqqq\bar{q}$ components in $N^*(1535)$ to the helicity amplitude $A_{1/2}^p$ and $S_{1/2}^p$

The next-to-next-to-lowest-energy configuration of the $qqqq\bar{q}$ components in $N^*(1535)$ is the one in which the flavor-spin configuration of the four quark subsystem has the mixed symmetry $[31]_{FS}[22]_F[31]_S$, as mentioned in section 2. For the same reason as that in section 3.2, the matrix element of the operator \hat{T}_A between the anti-quark states vanishes, and the diagonal contributions to $S_{1/2}^p$ is 0. The difference is, there are two $qqqq\bar{q}$ components in $N^*(1535)$ with the four quark flavor-spin configuration $[31]_{FS}[22]_F[31]_S$. Here we neglect the transitions $\gamma^* uudd \rightarrow uuds\bar{s}$ and $\gamma^* uuds\bar{s} \rightarrow uudd\bar{d}$. Calculation

leads to the result:

$$\begin{aligned} A_{1/2}^{p(5q')} &= -A_{(p)d\bar{d}} A_{(N^*)d\bar{d}} \frac{1}{\sqrt{2K_\gamma}} \frac{k_\gamma^2}{18\omega_5} \frac{e}{2m} \exp\left\{-\frac{k_\gamma^2}{5\omega_5^2}\right\} - \\ &\quad A_{(p)s\bar{s}} A'_{(N^*)s\bar{s}} \frac{1}{\sqrt{2K_\gamma}} \frac{k_\gamma^2}{12\omega_5} \left(\frac{e}{2m} - \frac{e}{6m_s}\right) \\ &\quad \times \exp\left\{-\frac{k_\gamma^2}{5\omega_5^2}\right\}, \\ S_{1/2}^{p5q'} &= 0. \end{aligned} \quad (29)$$

In the case of the annihilation transitions straightforward calculation leads to the result that the flavor-spin overlap factors for the transition $\gamma^* qqq \rightarrow qqqq\bar{q}$ C_{FS} vanish, both for $A_{1/2}^p$ and $S_{1/2}^p$. Therefore this transition does not contribute to the process $\gamma^* p \rightarrow N^*(1535)$.

The next step is to consider the contributions of the transitions $\gamma^* qqqq\bar{q} \rightarrow qqq$. The flavor-spin configuration for the four-quarks subsystem of the $qqqq\bar{q}$ components in the proton is $[4]_{FS}[22]_F[22]_S$, for which the explicit form has been given in Ref. [18]. After some calculation, it emerges that the flavor-spin overlap factors are also 0. Consequently, this process also yields no contribution to the transition $\gamma^* p \rightarrow N^*(1535)$.

Finally, we find that the the next-to-next-to-lowest-energy $qqqq\bar{q}$ components in $N^*(1535)$ does not contribute to the helicity amplitude $S_{1/2}^p$ for the electromagnetic transition $\gamma^* p \rightarrow N^*(1535)$. The contributions to $A_{1/2}^p$ only comes from the diagonal transition elements. As in the case of the contributions of the lowest energy $qqqq\bar{q}$ components, this contribution is also very small. And as the the non-diagonal contribution to $A_{1/2}^p$ is 0, this 5-quark component does not contribute significantly to the last results. The result, which contains all the contributions for $A_{1/2}^p$ that we have considered is shown in figure 5. For comparison, we have considered several different probabilities of the $qqqq\bar{q}$ components in $N^*(1535)$, as is discussed in details in section 3.5.

3.4 The helicity amplitude $A_{1/2}^n$ at the photon point

As we know, the ratio of the helicity amplitudes at photon point for proton and neutron is not a trivial issue. So we calculate the $A_{1/2}^n$ in this section. For isospin symmetry, the wave functions for neutron and $n^*(1535)$ can be obtained by the wave functions we have given for the proton and $p^*(1535)$. Consequently, we can calculate the matrix elements directly. After some calculations, we can get the following results:

$$\begin{aligned} A_{1/2}^{n(3q)} &= -A_{(p)3q} A_{(N^*)3q} \frac{1}{\sqrt{2K_\gamma}} \frac{e}{2m} \left(\frac{k_\gamma^2}{3\omega_3} + \frac{2\omega_3}{9}\right) \exp\left\{-\frac{k_\gamma^2}{6\omega_3^2}\right\} \\ A_{1/2}^{n(5q)} &= -A_{(p)s\bar{s}} A_{(N^*)s\bar{s}} \frac{1}{\sqrt{2K_\gamma}} \frac{\omega_5}{24} \left(\frac{e}{2m} + \frac{e}{2m_s}\right) \exp\left\{-\frac{k_\gamma^2}{5\omega_5^2}\right\} \\ A_{1/2}^{n(3q \rightarrow 5q)} &= -A_{(p)3} A_{(N^*)s\bar{s}} \frac{1}{\sqrt{2K_\gamma}} \frac{\sqrt{2}}{6} e C_{35} \exp\left\{-\frac{3k_\gamma^2}{20\omega_5^2}\right\}. \end{aligned} \quad (30)$$

As we can see in equation (30), the non-diagonal contributions to the helicity amplitude $A_{1/2}^n$ is same as the one to $A_{1/2}^p$. Note that here we have only considered the contributions of the lowest energy five-quark components in $n^*(1535)$, for that the probability of the next-to-next-to-lowest-energy $qqqq\bar{q}$ components should be some smaller, and on the other side, we can see in the section 3.3, the non-diagonal contributions between the three-quark component and this five-quark configuration is 0, so it may only give a very small correction to our result, so we can neglect it here.

If we set $\omega_3 = 340$ MeV, and the constituent quark masses are taken to be the same value as that in section 3.1, then we can get that $A_{1/2}^n = -0.123/\sqrt{\text{GeV}}$, which is much larger than the data $A_{1/2}^n = -0.046 \pm 0.027/\sqrt{\text{GeV}}$ [25]. It indicates that we should consider the contributions of the five-quark components. When the contributions of the $qqqq\bar{q}$ components are taken into account, with the same parameter employed in section 3.2 (That for the best fit), we can get that the helicity amplitude $A_{1/2}^n = -0.074/\sqrt{\text{GeV}}$, which falls in the range of the data. And the ratio $A_{1/2}^n/A_{1/2}^p$ is then -0.82 , which also falls well in the range of the data 0.84 ± 0.15 . Note that the non-diagonal contributions to $A_{1/2}^n$ is same as that to $A_{1/2}^p$, and as we have obtained in section 3.2 that this contribution should be the major one of the $qqqq\bar{q}$ components, so we can conclude that the ratio $A_{1/2}^n/A_{1/2}^p$ is not sensitive with the free parameter ω_5 .

3.5 The probabilities of the $qqqq\bar{q}$ components in $N^*(1535)$

Here we have calculated the helicity amplitude $A_{1/2}^p$ by considering all the contributions of the qqq and low lying $qqqq\bar{q}$ components in the proton and $N^*(1535)$. The last result is shown in figure 5 as a function of Q^2 . Here all the lines are obtained by taking $\omega_3 = 340$ MeV and $\omega_5 = 600$ MeV. The solid line is obtained by taking the probability of the lowest energy $qqqq\bar{q}$ components in $N^*(1535)$ to be the totally P_{5q} , and the dash dot line $0.6P_{5q}$ MeV, i.e. the probability of the next-to-next-to-lowest-energy $qqqq\bar{q}$ components is $0.4P_{5q}$, and both the two lines are obtained by setting $P_{3q} = 55\%$. The dot line is obtained by setting $P_{3q} = 35\%$, and the dash line $P_{3q} = 75\%$, and both of the two lines are obtained by taking the probability of the lowest energy $qqqq\bar{q}$ component to be the totally P_{5q} .

As shown in figure 5, the best description of $A_{1/2}^p$ is given by the curve obtained by taking the probability of the lowest energy $qqqq\bar{q}$ components in $N^*(1535)$ to be $P_{5q} = 45\%$. This indicates that this electromagnetic transition does not favor any large probability of the next-to-next-to-lowest energy $qqqq\bar{q}$ components in $N^*(1535)$, although its contribution is tiny and the result is not very sensitive to it. The main result is that if the probability of the lowest energy $5q$ components falls in the range 25-65% the calculated helicity amplitudes may fall within the data range $90 \pm 30/\sqrt{\text{GeV}}$ at the photon point.

4 Conclusion

The helicity amplitudes $A_{1/2}^p$ and $S_{1/2}^p$ for the electromagnetic transition $\gamma^*p \rightarrow N^*(1535)$ were calculated, and the possible role of the $qqqq\bar{q}$ was investigated. The results indicate that the extension of the qqq quark model to include $qqqq\bar{q}$ components can bring about a much better description of the empirical results. The results indicate that the admixtures of $qqqq\bar{q}$ components in the $N^*(1535)$ resonance might be in the range 25 – 65%, and about 20% in the proton.

The orbital-flavor-spin configuration of the four-quark subsystem in the $qqqq\bar{q}$ components of the proton was assumed to be $[31]_X[4]_{FS}[22]_F[22]_S$, a configuration which is expected to have the lowest energy, and therefore most likely to form appreciable components of the proton. In the case of the resonance $N^*(1535)$, the lowest energy configuration is $[4]_X[31]_{FS}[211]_F[22]_S$, which requires that the $5q$ component of $N^*(1535)$ should only be $s\bar{s}$ component. This means that there may be large strangeness components in $N^*(1535)$ resonance, which is consistent with the strong couplings of $N^*(1535)N\phi$ and $N^*(1535)K\Lambda$, predicted in Refs. [10] and [11]. This is also in line with the $K\Sigma$ quasibound state explanation for $N^*(1535)$ by the mechanism of dynamical resonance formation within the coupled channel approach based on chiral $SU(3)$ [3, 4, 5, 15]. In addition we considered the contributions of the $uudd\bar{d}$ and $uudu\bar{u}$ components in the $N^*(1535)$, which have the orbital-flavor-spin configuration $[4]_X[31]_{FS}[22]_F[31]_S$. The results show that this electromagnetic transition does not favor large $qqqq\bar{q}$ components with the next-to-next-to-lowest-energy.

The suggested large probability $s\bar{s}$ components in $N^*(1535)$, may be naturally consistent with the mass ordering of the resonances $N^*(1440)$ and $N^*(1535)$. For the Roper resonance, the largest $5q$ component is $uudd\bar{d}$ [9], while that for $N^*(1535)$ is $uuds\bar{s}$ component, which may make it heavier than the roper resonance. If we neglect higher energy configurations of the $qqqq\bar{q}$ components in these two resonances, the $s\bar{s}$ components in the Roper should be $P_{5q}/3$ [19], in the case of $N^*(1535)$, it is P_{5q} , which may make it heavier than the Roper resonance.

5 Acknowledgments

We are grateful to Professor D. O. Riska for helpful discussions and English editing of the draft, and Dr Q. B. Li for helpful discussions. This work is partly supported by the National Natural Science Foundation of China under grants Nos. 10435080, 10521003, and by the Chinese Academy of Sciences under project No. KJCX3-SYW-N2.

A The explicit form of the flavor-spin configuration $[31]_{FS}[211]_F[22]_S$

The explicit decomposition of the flavor-spin configuration $[31]_{FS}[211]_F[22]_S$ may be expressed as [23]

$$|[31]_{FS}\rangle_1 = \frac{1}{2} \{ \sqrt{2} |[211]\rangle_{F1} |[22]\rangle_{S1} - |[211]\rangle_{F2} |[22]\rangle_{S1} + |[211]\rangle_{F3} |[22]\rangle_{S3} \}, \quad (31)$$

$$|[31]_{FS}\rangle_2 = \frac{1}{2} \{ \sqrt{2} |[211]\rangle_{F1} |[22]\rangle_{S2} + |[211]\rangle_{F2} |[22]\rangle_{S2} + |[211]\rangle_{F3} |[22]\rangle_{S1} \}, \quad (32)$$

$$|[31]_{FS}\rangle_3 = \frac{1}{\sqrt{2}} \{ -|[211]\rangle_{F2} |[22]\rangle_{S2} + |[211]\rangle_{F3} |[22]\rangle_{S1} \}, \quad (33)$$

and the explicit forms of the flavor symmetry $[211]_F$ and spin symmetry $[22]_S$ are

$$|[211]\rangle_{F1} = \frac{1}{4} \{ 2|uuds\rangle - 2|usud\rangle - |duus\rangle - |udus\rangle - |sudu\rangle - |usdu\rangle + |suud\rangle + |dusu\rangle + |usud\rangle + |udsu\rangle \}, \quad (34)$$

$$|[211]\rangle_{F2} = \frac{1}{\sqrt{48}} \{ 3|udus\rangle - 3|duus\rangle + 3|suud\rangle - 3|usud\rangle + 2|dsuu\rangle - 2|sduu\rangle - |sudu\rangle + |usdu\rangle + |dusu\rangle - |udsu\rangle \}, \quad (35)$$

$$|[211]\rangle_{F3} = \frac{1}{\sqrt{6}} \{ |sudu\rangle + |udsu\rangle + |dsuu\rangle - |usdu\rangle - |dusu\rangle - |sduu\rangle \}, \quad (36)$$

$$|[22]\rangle_{S1} = \frac{1}{\sqrt{12}} \{ 2|\uparrow\uparrow\downarrow\downarrow\rangle + 2|\downarrow\downarrow\uparrow\uparrow\rangle - |\downarrow\uparrow\uparrow\downarrow\rangle - |\uparrow\uparrow\downarrow\downarrow\rangle - |\downarrow\uparrow\downarrow\uparrow\rangle - |\uparrow\downarrow\downarrow\uparrow\rangle \}, \quad (37)$$

$$|[22]\rangle_{S2} = \frac{1}{2} \{ |\uparrow\downarrow\uparrow\downarrow\rangle + |\downarrow\uparrow\downarrow\uparrow\rangle - |\downarrow\uparrow\uparrow\downarrow\rangle - |\uparrow\downarrow\downarrow\uparrow\rangle \} \quad (38)$$

B The explicit form of the flavor-spin configuration $[31]_{FS}[22]_F[31]_S$

The explicit decomposition of the flavor-spin configuration $[31]_{FS}[22]_F[31]_S$ may be expressed as [23]

$$|[31]_{FS}\rangle_1 = \frac{1}{\sqrt{2}} \{ |[22]\rangle_{F1} |[31]\rangle_{S2} + |[22]\rangle_{F2} |[31]\rangle_{S3} \} \quad (39)$$

$$|[31]_{FS}\rangle_2 = \frac{1}{2} \{ \sqrt{2} |[22]\rangle_{F1} |[31]\rangle_{S1} + |[22]\rangle_{F1} |[31]\rangle_{S2} - |[22]\rangle_{F2} |[31]\rangle_{S3} \}, \quad (40)$$

$$|[31]_{FS}\rangle_3 = \frac{1}{2} \{ \sqrt{2} |[22]\rangle_{F2} |[31]\rangle_{S1} - |[22]\rangle_{F2} |[31]\rangle_{S2} - |[22]\rangle_{F1} |[31]\rangle_{S3} \}, \quad (41)$$

the explicit forms of the flavor symmetry $[22]_F$ has been shown in Ref. [18], and spin symmetry $[31]_S$ may be (for

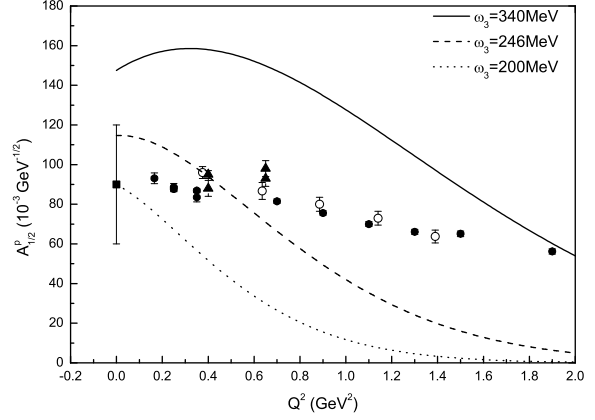


Fig. 1. The helicity amplitude $A_{1/2}^p$ for $\gamma^* p \rightarrow N^*(1535)$ in the qqq model. Here the solid line is obtained by taking $\omega_3 = 340$ MeV, and the dash and dot lines are obtained by taking $\omega_3 = 246$ MeV and $\omega_3 = 200$ MeV, respectively. The data point at $Q^2 = 0$ (square) is from Ref. [25], the other points are taken from Ref. [26] (triangles), [27] (open circles) and [28] (filled circles).

$S_z = +1$)

$$|[31]\rangle_{S1} = \frac{1}{\sqrt{12}} \{ 3|\uparrow\uparrow\uparrow\downarrow\rangle - |\uparrow\uparrow\downarrow\uparrow\rangle - |\uparrow\downarrow\uparrow\uparrow\rangle - |\downarrow\uparrow\uparrow\uparrow\rangle \}, \quad (42)$$

$$|[31]\rangle_{S2} = \frac{1}{\sqrt{6}} \{ 2|\uparrow\uparrow\downarrow\uparrow\rangle - |\uparrow\downarrow\uparrow\uparrow\rangle - |\downarrow\uparrow\uparrow\uparrow\rangle \}, \quad (43)$$

$$|[31]\rangle_{S3} = \frac{1}{\sqrt{2}} \{ |\uparrow\downarrow\uparrow\uparrow\rangle - |\downarrow\uparrow\uparrow\uparrow\rangle \}, \quad (44)$$

(for $S_z = 0$)

$$|[31]\rangle_{S1} = \frac{1}{\sqrt{6}} \{ |\uparrow\uparrow\downarrow\downarrow\rangle + |\downarrow\uparrow\uparrow\downarrow\rangle + |\uparrow\downarrow\uparrow\downarrow\rangle - |\downarrow\downarrow\uparrow\uparrow\rangle - |\uparrow\downarrow\downarrow\uparrow\rangle - |\downarrow\downarrow\uparrow\uparrow\rangle \}, \quad (45)$$

$$|[31]\rangle_{S2} = \frac{1}{\sqrt{12}} \{ 2|\uparrow\uparrow\downarrow\downarrow\rangle - 2|\downarrow\downarrow\uparrow\uparrow\rangle + |\uparrow\downarrow\uparrow\uparrow\rangle - |\downarrow\uparrow\uparrow\downarrow\rangle + |\downarrow\downarrow\uparrow\uparrow\rangle - |\uparrow\downarrow\uparrow\downarrow\rangle \}, \quad (46)$$

$$|[31]\rangle_{S3} = -\frac{1}{2} \{ |\downarrow\uparrow\uparrow\downarrow\rangle - |\uparrow\downarrow\uparrow\uparrow\rangle + |\downarrow\uparrow\downarrow\uparrow\rangle - |\uparrow\downarrow\uparrow\downarrow\rangle \} \quad (47)$$

References

1. S. Capstick and N. Isgur, Phys. Rev. **D34** (1986)2809
2. L.Ya. Glozman and D. O. Riska, Phys. Rept. **268** (1996) 263
3. N. Kaiser, P. Siegel and W. Weise, Phys. Lett. **B362** (1995) 23
4. D. Jido et al., Nucl. Phys. **A725** (2003) 181
5. D. Jido, M. Döring and E. Oset, Phys. Rev. **C77** (2008) 065207.

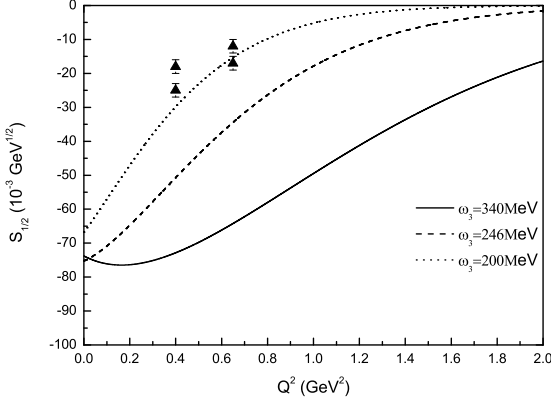


Fig. 2. The helicity amplitude $S_{1/2}^p$ for $\gamma^* p \rightarrow N^*(1535)$ in the qqq model. The data points are extracted from Ref. [26].

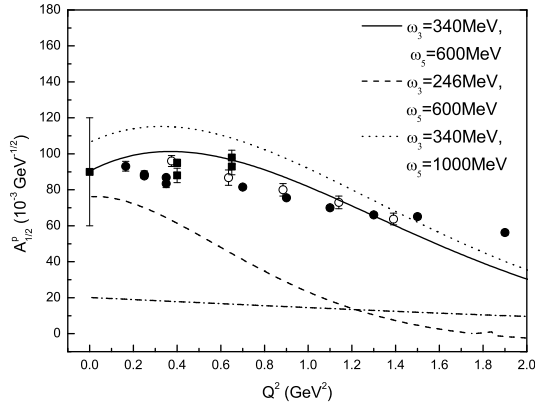


Fig. 3. The helicity amplitude $A_{1/2}^p$ for $\gamma^* p \rightarrow N^*(1535)$ contains the contributions both of the qqq and lowest energy $qqqq\bar{q}$ components in the proton and $N^*(1535)$. Here the solid line is obtained by taking $\omega_3 = 340$ MeV and $\omega_5 = 600$ MeV, the dash line $\omega_3 = 246$ MeV and $\omega_5 = 600$ MeV, and the dot line $\omega_3 = 340$ MeV and $\omega_5 = 1000$ MeV, respectively. And the dash dot line is the absolute value of the contributions of the 5-quark component with $\omega_3 = 340$ and $\omega_5 = 600$ MeV. Data point as in figure 1.

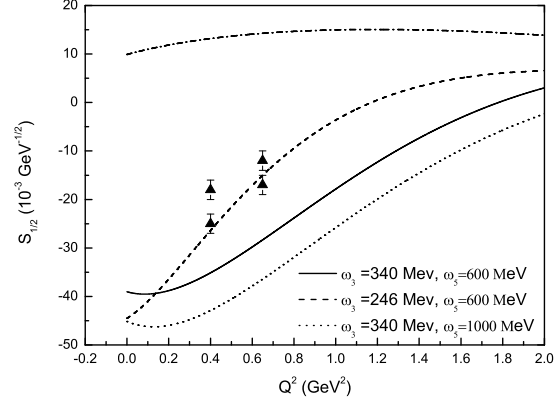


Fig. 4. The helicity amplitude $S_{1/2}^p$ for $\gamma^* p \rightarrow N^*(1535)$ contains the contributions both of the qqq and lowest energy $qqqq\bar{q}$ components in the proton and $N^*(1535)$. The dash dot line is the empirical value of the contributions of the 5-quark component with $\omega_3 = 340$ and $\omega_5 = 600$ MeV. Data point as in figure 2.

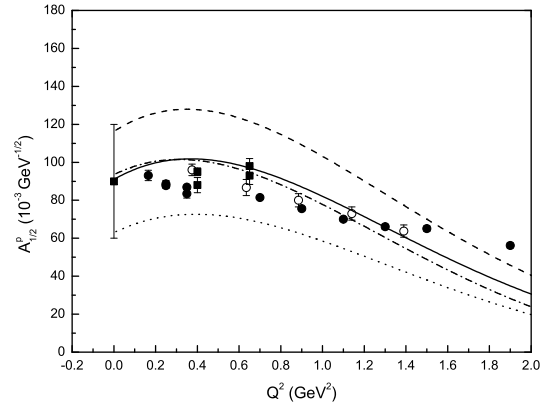


Fig. 5. The total helicity amplitude $A_{1/2}^p$ for $\gamma^* p \rightarrow N^*(1535)$. Here all the lines are obtained by taking $\omega_3 = 340$ MeV and $\omega_5 = 600$ MeV. The solid line is obtained by taking the probability of the lowest energy $qqqq\bar{q}$ components in $N^*(1535)$ to be the totally P_{3q} , and the dash dot line $0.6P_{3q}$ MeV, i. e. the probability of the next-to-next-to-lowest energy $qqqq\bar{q}$ components is $0.4P_{3q}$, and both the two lines are obtained by setting $P_{3q} = 0.55$. The dot line is obtained by setting $P_{3q} = 0.35$, and the dash line $P_{3q} = 0.75$, and both of the two lines are obtained by taking the probability of the lowest energy $qqqq\bar{q}$ component to be the totally P_{3q} . Data point as in figure 1.

6. S. Capstick, B. D. Keister and D. Morel, J. Phys. Conf. Ser. **69** (2007) 012016
7. Q. B. Li and D. O. Riska, Nucl. Phys. **A766** (2006) 172
8. Q. B. Li and D. O. Riska, Phys. Rev. **C73** (2006) 035201
9. Q. B. Li and D. O. Riska, Phys. Rev. **C74** (2006) 015202
10. J. J. Xie, B. S. Zou and H. C. Chiang, Phys. Rev. **C77** (2008) 015206
11. B. C. Liu and B. S. Zou, Phys. Rev. Lett. **96** (2006) 042002
12. S. Capstick and W. Roberts, Pro. Par. Nucl. Phys. **45** (2000) S241
13. V. D. Burkert, Pro. Par. Nucl. Phys. **55** (2005) 108
14. C. Helminen and D. O. Riska, Nucl. Phys. **A699** (2002) 624
15. N. Kaiser, T. Waas and W. Weise, Nucl. Phys. **A612** (1997) 297

16. M. Döring, E. Oset and B.S. Zou, Phys. Rev. **C78** (2008) 025207
17. B. S. Zou and D. O. Riska, Phys. Rev. Lett. **95** (2005) 072001
18. C. S. An, D. O. Riska and B. S. Zou, Phys. Rev. **C73** (2006) 035207
19. C. S. An, Q. B. Li, D. O. Riska and B. S. Zou, Phys. Rev. **C74** (2006) 055205, Erratum-ibid. **C79** (2007) 069901

20. C. S. An, Nucl. Phys. **A797** (2007) 131 , Erratum-
ibid.**A801** (2008) 82
21. C. S. An and D. O. Riska, Eur. Phys. J. **A37** (2008) 263
22. B. Juliá-Díaz, T.-S. H. Lee, T. Sato and L. C. Smith, Phys.
Rev. **C75** (2007) 015205
23. J. Q. Chen, *Group Representation Theory for Physi-*
cists, 2nd edition (World Scientific, Singapore, 1989)
24. R. Koniuk and N. Isgur, Phys. Rev. **D21** (1980) 1868,
Erratum-ibid.**D23** (1981) 818
25. Particle Group Data, J. Phys. **G33** (2006) 1
26. I. G. Aznauryan et al., Phys. Rev. **C71** (2005) 015201
27. The CLAS Collaboration, Phys. Rev. Lett. **86** (2001) 1702
28. The CLAS Collaboration, Phys. Rev. **C76** (2007) 015204